Instability in Low-Temperature Molecular-Beam Epitaxy Growth of Si/Si(111)

H.-N. Yang, G.-C. Wang, and T.-M. Lu
Department of Physics, Applied Physics and Astronomy, Rensselaer Polytechnic Institute, Troy, New York 12180-3590

(Received 23 June 1994)

Using high-resolution low-energy electron diffraction we studied *in situ* low-temperature molecular-beam epitaxial growth of Si/Si(111). At ~275 °C and a deposition rate of ~7 bilayers/min, a roughening evolution occurs after an initial transient layer-by-layer growth. It shows dynamic scaling characteristics with a roughness exponent $\alpha \approx 1$ and an interface growth exponent $\beta \approx \frac{1}{4}$. More importantly, the average local slope is found to increase with time as $\sim\sqrt{\ln(t)}$. However, such a roughening behavior does not exist either at temperatures higher than 350 °C or under a slower deposition rate of ~1 bilayer/min. The phenomena are consistent with a statistical model of linear diffusion dynamics.

PACS numbers: 64.60.Ht, 61.14.Hg, 68.55.Jk

The molecular-beam epitaxy (MBE) process has been widely studied for decades due to its technological importance and scientific interest. Recently, there has been considerable effort in understanding the mechanism of instability in which a rough growth front is generated. Two mechanisms have been proposed based on different driving forces: one from statistical fluctuation [1–8] and another one from asymmetric diffusion barrier in step edges [6,9,10]. In the statistical model, a rough surface is generated by the flux fluctuation. Because of competition between fluctuation and relaxation, the growing surface exhibits dynamic scaling characteristics with a steady evolution in both vertical roughening and lateral coarsening [1]. The local slope of the rough surface may or may not increase as a function of time, depending on whether nonlinear diffusion plays a role. On the other hand, in the step barrier model, unstable growth occurs when a step-edge diffusion barrier (Schwöbel barrier [11]) resists the landing atoms from downward migration. Large-scale mounds are formed on a singular surface with a stationary slope [10]. Both types of roughening structures seem to have been obtained in experiments [10,12–19], although the data available were far from complete.

In this Letter, we report a study on *in situ* low-temperature molecular-beam epitaxial (MBE) growth of Si on a singular Si(111) surface using high-resolution low-energy electron diffraction (HRLEED) [20]. The technique is not only sensitive to local surface roughness but is also capable of resolving a small inclination angle down to 0.05° for surface structures having miscut, mosaic, or mounds at both large and small scales. We observed that roughening evolution with dynamic scaling characteristics occurs under a deposition rate of ~7 bilayers/min and at 275 ± 5 °C (Si melting temperature = 1410 °C). More importantly, the average local slope was found to increase with time proportional to $\sqrt{\ln(t)}$. However, such roughening behavior was not observed either at a slower deposition rate of ~1 bilayer/min or at temperatures higher than 350 °C, where for both cases, the ultimate angles for average slopes were measured to be relatively small (<0.6°). The phenomena are explained by a statistical fluctuation model under linear diffusion dynamics [3–8].

The experiment was performed in a UHV chamber equipped with a HRLEED system [20] and a Si evaporator. The Si evaporator is a compact rod-fed e^- beam source heated by electron bombardments to the tip of a Si rod, which provides a clean and controlled Si flux [21]. A flat Si(111) sample (~6 × 11 mm^2) with a miscut angle <0.1° and an average terrace width of at least 1000 Å was cleaned in UHV by flashing the sample up to 1200 °C. The substrate temperature was measured by a type-*C* thermocouple (W-5%Re vs W-26%Re). The growth processes were studied as functions of deposition time, growth rate, and substrate temperature. The surface steps created during deposition are biatomic (bilayer) steps as determined from out-of-phase diffraction conditions of HRLEED [22].

We first monitored the HRLEED intensity as a function of deposition time at different temperatures with a deposition rate of ~7 bilayers/min. Each data (beam intensity profile) was taken from the sample where the deposition was performed continuously to the time indicated, and the measurement was done after the sample was quenched to room temperature. Every deposition started from a clean and flat surface prepared by high-temperature flashing. Figures 1(a) and 1(b) show the time-dependent line shapes of the (00) beam intensity scanned along the $[\bar{1}\bar{1}2]$ direction at growth temperatures, 350 ± 5 °C, respectively. The data were taken at electron energy $E = 47.0$ eV, which corresponds to a near out-of-phase condition, $k_\perp c \approx 7.01\pi$, where c is the bilayer step height (3.135 Å) of Si(111). $k_\parallel$ and $k_\perp$ are the components of diffraction momentum transfers parallel and perpendicular to the surface, respectively. Note that [22] the diffraction technique is not sensitive to surface steps when constructive interference occurs at the in-phase conditions $k_\perp c = 2m\pi$ $(m = 0, 1, 2, \ldots)$. However, away from the in-phase conditions $k_\perp c \neq 2m\pi$,

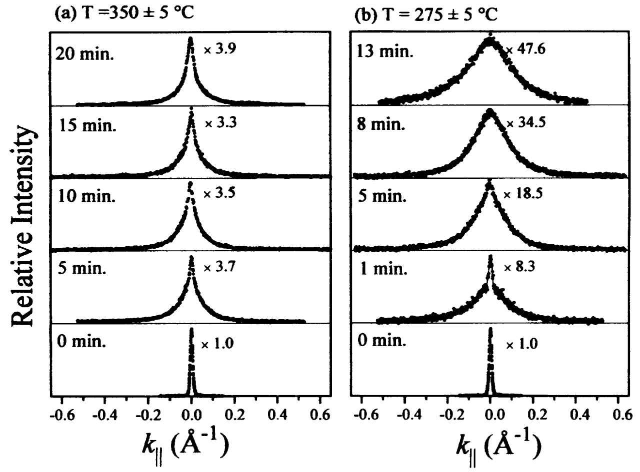

FIG. 1. Time-dependent angular profiles of the (00) beam scanned along the $[\bar{1}12]$ direction for the out-of phase condition, $k_{\perp}c \approx 7\pi$, are plotted at (a) 350 ± 5 °C and (b) 275 ± 5 °C, respectively. The deposition rate was fixed at ~7 bilayers/min. The relative intensity has been scaled up by the factor shown near the peak of each profile.

where destructive interference occurs, the steps can be detected from the broadened diffraction line shape. The broadening reaches maximum at the out-of-phase conditions $k_{\perp}c = (2m + 1)\pi$. As shown in Fig. 1, at $t = 0$ (before deposition), the line shapes exhibit a sharp δ-like profile that is identical to the HRLEED resolution. The Si(111) surface we used was therefore step free within the instrument response. Once the deposition proceeded, a diffuse profile built up and was superimposed to the central δ component, as demonstrated in Fig. 1(a) for $t > 0$ and in Fig. 1(b) at $t = 1$ min.

The "δ + diffuse" line shape is a characteristic of the surface containing steps with a finite interface width w [2,23], where w is the root-mean-square height fluctuation (in units of c). Because of coherent electron diffraction, a sharp central δ peak appears when the surface looks smooth on large scale, and it decays quickly with increasing w as $e^{-w^2(k_{\perp}c-2m\pi)^2}$, where $|k_{\perp}c - 2m\pi| \leq \pi$. The broad diffuse line shape is a result of the interference from local steps. In Fig. 1(a), at the longest deposition time, 20 min, for which about 140 bilayers were deposited, the δ component shows only little decay. The persistence of the δ component at out-of-phase conditions is an indication that the existing steps were restricted only to one or two levels of the surface [24]. Such a smooth morphology during growth at 350 °C was consistent with the previous experiments where the layer-by-layer growth was observed to last for quite a long time [25,26].

In contrast to the process at 350 °C, the growth at a lower temperature (~275 °C) exhibited a distinctly different behavior. Figure 2 is the plot of the time-dependent peak intensities measured within the first 100 s of deposition. Showing a damped oscillation at the initial stage, the intensity oscillation no longer existed after $t = 2$ min.

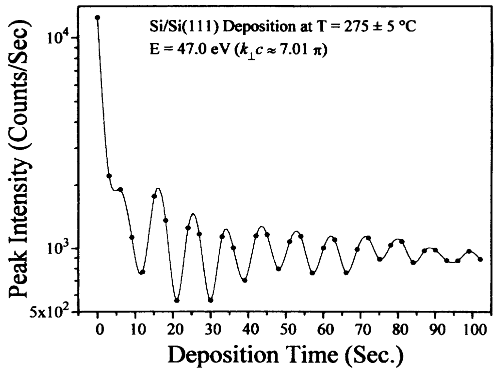

FIG. 2. Under a deposition rate of ~7 bilayers/min and at a sample temperature of 275 ± 5 °C, the damped intensity oscillations were observed within the first 100 s at $E = 47$ eV. The solid circles are experimental data points.

The δ intensity was also reduced significantly due to the increase of w. For longer times, $t > 4$ min, as shown in Fig. 1(b), the δ component completely disappeared. The growing surface thus developed into a multilayer rough structure. Quantitatively, we can estimate w from the ratio R of the integrated δ intensity to the total integrated intensity at the near in-phase conditions for which the δ component could still be measured. This ratio has a simple relation [2,23], $R \approx e^{-w^2(k_{\perp}c-2m\pi)^2}$, or $-\ln(R) = w^2|k_{\perp}c - 2m\pi|^2 \propto w^2$. In Fig. 3, we plot $-\ln(R)$ vs t at $|k_{\perp}c - 8\pi| = 0.349\pi$, a near in-phase condition. At $t = 10$ min, the thickness h of the deposited film was about 70 bilayers (≈220 Å) and the w reached $1.9c$ (≈6.0 Å). At 17 min, $h \approx 370$ Å and $w \approx 2.8c \approx 8.8$ Å. The systematic increase of w with time is thus a clear indication of the roughening evolution during growth.

From Fig. 1(b), one can further observe the continuous broadening of the diffuse profile as a function of time. Such broadening also occurred at other diffraction

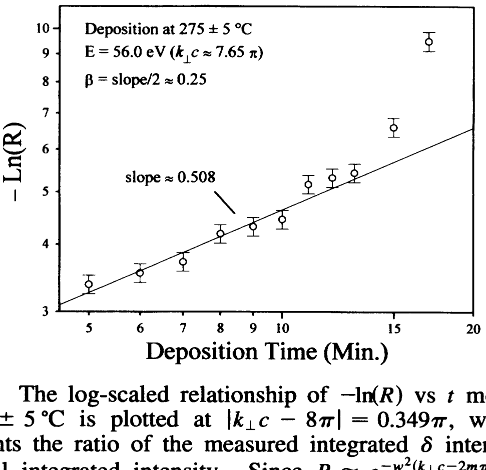

FIG. 3. The log-scaled relationship of $-\ln(R)$ vs t measured at 275 ± 5 °C is plotted at $|k_{\perp}c - 8\pi| = 0.349\pi$, where R represents the ratio of the measured integrated δ intensity to the total integrated intensity. Since $R \approx e^{-w^2(k_{\perp}c-2m\pi)^2}$, i.e., $-\ln(R) \propto w^2$, this plot actually shows the relationship between w^2 and t.

conditions, except near in-phase regions. Figure 4(a) is the log-scaled plot of the full width at half maximum (FWHM) of the diffuse line shapes as a function of $k_\perp c$ at different times, with $k_\perp c$ varying from 7.0 to 7.75π. Note that the FWHM is proportional to the average local slope or the average step density in a rough surface [2,23]. To demonstrate the evolution of the local slope during growth, we show in Fig. 4(b) a plot of FWHM vs t at a near out-of-phase condition of $E = 48$ eV, corresponding to $k_\perp c \approx 7.08\pi$.

We must point out that the observed roughening evolution is purely a dynamic phenomenon, which was not observed in previous studies of the Si/Si(111) system in similar temperature regions. The low temperature and the deposition conditions could be very crucial. For a comparison, we also studied a sevenfold slower process at 275 ± 5 °C with a deposition rate of ~1 bilayer/min. The roughening did not occur at this growth condition, and a smooth morphology similar to that observed at 350 °C was again observed.

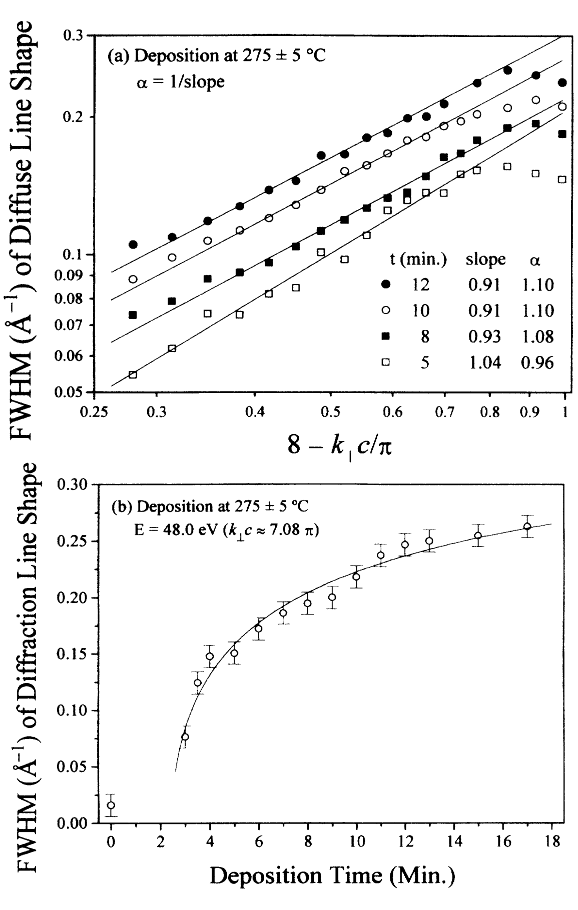

FIG. 4. (a) The log-scaled plots of FWHM vs $8 - k_\perp c/\pi$ along the $[\bar{1}12]$ direction for the (00) beam are shown at different growth times with the growth temperature 275 ± 5 °C. The uncertainty is about the size of the data points. The log-scaled linear relations indicate that the FWHM varies with $8 - k_\perp c/\pi$ in a form of power law. (b) The amplitude of FWHM at $k_\perp c = 7.08\pi$ is plotted as a function of the growth time in open circles. The solid curve results from the fitted results using the form of FWHM $= A\sqrt{\ln(t/\tau)}$.

The dynamic roughening shown above can be analyzed in the spirit of dynamic scaling principles based on the Wolf-Villain-Das Sarma (WVDS) model, a statistical model under linear diffusion dynamics [3–8]. The dynamic scaling theory predicted that, due to the fluctuation, the surface height-height correlation, $H(\mathbf{r},t) = \langle[z(\mathbf{r},t) - z(0,t)]^2\rangle$, has power-law relations both in space and time, where $z(\mathbf{r},t)$ is the surface height of an atom at the planar position $\mathbf{r}$. In the WVDS model in which a local linear diffusion mechanism was assumed to dominate the MBE growth, time scaling will exist on the long-range scale as $H(\mathbf{r},t) = 2w^2 \sim t^{1/2} \sim t^{2\beta}$, with the growth exponent $\beta = 0.25$. On the other hand, space scaling will exist on the short-range scale as $H(\mathbf{r},t) \sim r^2 \ln(t) \sim (\rho r)^{2\alpha}$, where the roughness exponent $\alpha = 1$ and the average local slope $\rho \propto \sqrt{\ln(t)}$ [8].

In linear diffusion dynamics, the local slope $[\propto \sqrt{\ln(t)}]$ is not stationary. This phenomenon arises from the fact that under sufficiently low temperatures or fast depositions, the atomic mobility is so low that the disordered atoms can only relax to nearby kink sites before subsequent deposited atoms arrive. The diffusion of atoms is thus unable to compete with the fluctuations, and the local slope will increase with time. This qualitatively agrees with the observation shown in Fig. 4. Quantitatively, we can show that the evolution of the slope does follow the simple $\sqrt{\ln(t)}$ growth law. The experimental data in Fig. 4(b) were fitted by an equivalent form, FWHM $= A\sqrt{\ln(t/\tau)}$, where A and τ are adjustable fitting parameters (the constant τ has a unit of time). The fit result is plotted as the solid curve in Fig. 4(b), which is reasonably good except at the initial transient layer-by-layer growth region $t < 2$ min. [The equation $\sqrt{\ln(t/\tau)}$ makes sense only for $t > \tau \sim 2.5$ min, so that the fit fails for $t < \tau$.]

The power-law type of height-height correlation, $H(\mathbf{r},t) \sim (\rho r)^{2\alpha}$ with $\alpha = 1$, can be further tested in the present experiment. We have shown rigorously [2,23] that, for a real-space power-law correlation, $H(r,t) \sim (\rho r)^{2\alpha}$, the reciprocal-space relationship, FWHM vs $k_\perp c$, should also exhibit a power-law, FWHM $\sim \rho|k_\perp c - 2m\pi|^{1/\alpha}$. As shown in Fig. 4(a), the plots at different times have the log-scaled linear relations, except at the region close to the out-of-phase condition, $k_\perp c \sim 7\pi$, i.e., $8 - k_\perp c/\pi \sim 1$. (The deviation at near the out-of-phase conditions is a result of the discrete lattice effect [2,23].) The FWHM thus varies with $8 - k_\perp c/\pi$ in a form of power law. Such a power-law relation is preserved for different times despite the continuous increase of the FWHM amplitude with time as $\sim\sqrt{\ln(t)}$. According to the linear relation $\log(\text{FWHM}) \sim \alpha^{-1} \log|8 - k_\perp c/\pi|$, the value of α was extracted from the slopes in Fig. 4(a) to be 1.03 ± 0.07. We conclude that the short-range height-height correlation measured from the present experiment is consistent with the form $H(\mathbf{r},t) \sim r^2 \ln(t)$.

The time scaling for interface width can be also examined from Fig. 3. Since the log-scaled plot in Fig. 3 shows a linear relation at $t \leq 13$ min, one obtains a power-law relation $w^2 \propto t^{2\beta}$. The growth exponent β can then be extracted from the slope to be $\beta = 0.25 \pm 0.02$. The result at $t \leq 13$ min thus agrees reasonably with the prediction by linear diffusion dynamics. To understand the crossover behavior in the later growth stage of $t \geq 15$ min, as shown in the anomalous increase of w from Fig. 3, we monitored the intensity as a function of t and found that it started to decay much faster even at the in-phase conditions. After $t = 25$ min, the intensity had become too low to be measured. Such a strong disorder is usually related to the formation of an amorphous type of defect structure in the surface, which has been confirmed in the previous experiments [15] where the interface width was found to grow much faster in the thicker amorphous Si film.

The present result is very different from our previous experiment of Fe/Fe(100) epitaxial growth [13], in which the local slope (ρ) became stationary (independent of time) in the final stage. In that case, nonlinear dynamics played an important role, and the fluctuation and diffusion came to a balance so that a constant value of ρ was achieved. Our observation also differs from a recent experiment on Cu/Cu(100) which was more consistent with the Schwöbel barrier model because the pyramidlike structures with a stationary slope were produced during growth [16]. It thus appears that for the Si/Si(111) system, in the low temperature (275 °C) fast growth case, the roughening evolution with growing local slope is driven by statistical fluctuation rather than the Schwöbel effect. Even for the two smooth growth cases, namely, the slower growth at 275 °C or faster growth at 350 °C, the results did not appear to be consistent with the Schwöbel barrier model. We have calculated the average slopes for these two cases, where the line shapes show a slight broadening. From the measured FWHM, we estimate that the local slopes of growing surface are quite small, corresponding to an ultimate angle less than 0.6°. Therefore, the large-scale mounds occurring in the GaAs growth with angles of a few degrees [10] are not observed in the present system. Based on the observed dynamic scaling characteristics in both space and time, especially the measured $\sqrt{\ln(t)}$ law in the growth of local slope, we believe that our present result is the first complete experimental confirmation for MBE growth that is dominated by the linear diffusion mechanism.

This work is supported by NSF under Grant No. 9213023.

---

[1] For review, see, *Dynamics of Fractal Surfaces,* edited by F. Family and T. Vicsek (World Scientific, Singapore, 1990), and references therein.

[2] H.-N. Yang, T.-M. Lu, and G.-C. Wang, *Diffraction from Rough Surfaces and Dynamic Growth Fronts* (World Scientific, Singapore, 1993).

[3] D.E. Wolf and J. Villain, Europhys. Lett. **13**, 389 (1990).

[4] Z.-W. Lai and S. Das Sarma, Phys. Rev. Lett. **66**, 2348 (1991).

[5] L.-H. Tang and T. Nattermann, Phys. Rev. Lett. **66**, 2899 (1991).

[6] A. Zangwill, D.D. Vvedensky, C.N. Luse, and M.R. Wilby, Surf. Sci. **274**, L529 (1992); Phys. Rev. E **48**, 852 (1993).

[7] M. Siegert and M. Plischke, Phys. Rev. Lett. **68**, 2035 (1992).

[8] J.G. Amar, P.-M. Lam, and F. Family, Phys. Rev. E **47**, 3242 (1993); J.G. Amar and F. Family, in *Mechanisms of Thin Film Evolution,* edited by S.M. Yalisove, C.V. Thompson, and D.J. Eaglesham, MRS Symposia Proceedings No. 317 (Materials Research Society, Pittsburgh, 1994).

[9] J. Villain, J. Phys. I (France) **1**, 19 (1991).

[10] M.D. Johnson, C. Orme, A.W. Hunt, D. Graff, J. Sudijono, L.M. Sander, and B.G. Orr, Phys. Rev. Lett. **72**, 116 (1994).

[11] R.L. Schwöbel, J. Appl. Phys. **40**, 614 (1969).

[12] J. Chevrier, V. Le Thanh, R. Buys, and J. Derrien, Europhys. Lett. **16**, 732 (1991).

[13] Y.-L. He, H.-N. Yang, T.-M. Lu, and G.-C. Wang, Phys. Rev. Lett. **69**, 3770 (1992).

[14] J. Krim, I. Heyvaert, C. Van Haesendonck, and Y. Bruynseraede, Phys. Rev. Lett. **70**, 57 (1993).

[15] D.L. Eaglesham, H.-J. Gossmann, and M. Cerullo, Phys. Rev. Lett. **65**, 1227 (1990); D.L. Eaglesham and G.H. Gilmer, in *Surface Disordering: Growth, Roughening and Phase Transitions,* edited by R. Jullien *et al.* (Nova, New York, 1993).

[16] H.-J. Ernst, F. Fabre, R. Folkerts, and J. Lapujoulade, Phys. Rev. Lett. **72**, 112 (1994).

[17] W.M. Tong, R.S. Williams, A. Yanase, Y. Segawa, and M.S. Anderson, Phys. Rev. Lett. **72**, 3374 (1994).

[18] H. Zeng and G. Vidali, in Proceedings of the 54th PEC Conference, Knoxville, 1994 (unpublished).

[19] D.Y. Noh, S. Chandavarkar, Y. Hwu, Z. Fu, and K.S. Liang, in Proceedings of the 54th PEC Conference, Knoxville, 1994 (Ref. [18]).

[20] U. Scheithauer, G. Meyer, and M. Henzler, Surf. Sci. **178**, 441 (1986); J.-K. Zuo, R.A. Harper, and G.-C. Wang, Appl. Phys. Lett. **51**, 250 (1987).

[21] B.T. Jonker, J. Vac. Sci. Technol. A **8**, 3883 (1990).

[22] T.-M. Lu and M.G. Lagally, Surf. Sci. **120**, 47 (1982).

[23] H.-N. Yang, T.-M. Lu, and G.-C. Wang, Phys. Rev. Lett. **68**, 2612 (1992); Phys. Rev. B **47**, 3911 (1993).

[24] C.S. Lent and P.I. Cohen, Surf. Sci. **139**, 121 (1984); J.M. Pimbley and T.-M. Lu, J. Vac. Sci. Technol. A **2**, 457 (1984); H.-N. Yang, K. Fang, T.-M. Lu, and G.-C. Wang, Europhys. Lett. **19**, 215 (1992).

[25] J. Aarts and P.K. Larsen, Surf. Sci. **188**, 391 (1987).

[26] R. Altsinger, H. Busch, M. Horn, and M. Henzler, Surf. Sci. **200**, 235 (1988).